

# Diverse frequency band-based convolutional neural networks for tonic cold pain assessment using EEG

Mingxin Yu<sup>a,b</sup>, Yichen Sun<sup>a</sup>, Bofei Zhu<sup>a</sup>, Lianqing Zhu<sup>a,\*</sup>, Yingzi Lin<sup>b,\*</sup>, Xiaoying Tang<sup>c</sup>, Yikang Guo<sup>b</sup>, Guangkai Sun<sup>a</sup>, Mingli Dong<sup>a</sup>

<sup>a</sup> Key Laboratory of the Ministry of Education for Optoelectronic Measurement Technology and Instrument, Beijing Information Science and Technology University, 6 Hongxia Road, Chaoyang District, Beijing 100015, China

<sup>b</sup> Intelligent Human-Machine Systems Lab, College of Engineering, Northeastern University, 360 Huntington Ave., Boston, MA 02115, USA

<sup>c</sup> School of Life Sciences, Beijing Institute of Technology, 5 Zhongguancun South Street, Haidian District, Beijing 100086, China

## ARTICLE INFO

### Article history:

Received 23 December 2018

Revised 19 September 2019

Accepted 13 October 2019

Available online 17 October 2019

Communicated by Dr. Li Sheng

### Keywords:

Tonic cold pain classification

EEG

Convolutional Neural Networks (ConvNets)

Deep learning

Pattern recognition

## ABSTRACT

The purpose of this study is to present a novel classification framework, called diverse frequency band-based Convolutional Neural Networks (DFB-based ConvNets), which can objectively identify tonic cold pain states. To achieve this goal, scalp EEG data were recorded from 32 subjects under cold stimuli conditions. The proposed DFB-based ConvNets model is capable of classifying three classes of tonic pain: No pain, Moderate Pain, and Severe Pain. Firstly, the proposed method utilizes diverse frequency band-based inputs to learn temporal representations from different frequency bands of Electroencephalogram (EEG) which are expected to have more discriminative power. Then the derived features are concatenated to form a feature vector, which is fed into a fully-connected network for performing the classification task. Experimental results demonstrate that the proposed method successfully discriminates the tonic cold pain states. To show the superiority of the DFB-based ConvNets classifier, we compare our results with the state-of-the-art classifiers and show it has a competitive classification accuracy (97.37%). Moreover, these promising results may pave the way to use DFB-based ConvNets in clinical pain research.

© 2019 Elsevier B.V. All rights reserved.

## 1. Introduction

Pain management is one of the essential goals in health and patient care. It is directly related to (1) patient safety, (2) therapeutic effectiveness, and (3) patient's positive experience. Generally, clinicians rely on patients' self-reported information as well as assessments of multiple clinical cues. In practical settings, the most common measures available for pain assessment are visual analog scales (VAS), numerical rating scales (NRS), and verbal rating scales (VRS) [1]. Self-reported measures are considered the gold standard for helping physicians and caregivers guide treatment accurately. Although it is a fact that self-report measures are able to provide important clinical information for pain patients, those approaches fail to be used with some individuals who are unable to verbally give their pain intensity, such as infants, patients with disorders of

consciousness, and demented patients [2,3]. Additionally, some patients who are addicted to drugs give false information about their pain intensity on purpose to obtain medication. By nature, scores based on patients' responses are not suitable for frequent administration, to assess pain continuously for trends over time or for continuous patient monitoring. The consequences of inadequate and delayed pain assessment include misdiagnosis, inappropriate treatment, patient dissatisfaction and increased patient risks [43,44]. Consequently, objective measurement of pain has long been clinicians' Holy Grail for effective pain treatment and management.

Pain is a complex unpleasant experience and a sign or symptom associated with real or potential tissue damage or illness [4]. The response of pain perception can either reflect sensory information, or can be influenced by various social and psychological factors [5]. Hence, pain is regarded as a multi-dimensional complex phenomenon. Although pain is considered an important factor in patient care, few methods are available to clinicians for objective assessment of pain [6,7]. In past years, many researchers were seeking to take advantage of neuroimaging techniques for pain intensity measurement including single-photon emission tomography (SPET) [40], positron emission tomography (PET) [41], functional magnetic tomography imaging (fMRI) [42], and elec-

\* Corresponding authors.

E-mail addresses: [mingxinbit@gmail.com](mailto:mingxinbit@gmail.com) (M. Yu), [sunyichen0429@163.com](mailto:sunyichen0429@163.com) (Y. Sun), [bofeizhubistu@163.com](mailto:bofeizhubistu@163.com) (B. Zhu), [lianqingzhubistu@163.com](mailto:lianqingzhubistu@163.com), [yumingxin@bistu.edu.cn](mailto:yumingxin@bistu.edu.cn) (L. Zhu), [yilin@coe.neu.edu](mailto:yilin@coe.neu.edu) (Y. Lin), [tangxiaoyingbitlife@gmail.com](mailto:tangxiaoyingbitlife@gmail.com) (X. Tang), [yikanguo@sohu.com](mailto:yikanguo@sohu.com) (Y. Guo), [guangkai\\_sun@sohu.com](mailto:guangkai_sun@sohu.com) (G. Sun), [minglibistu@sina.com](mailto:minglibistu@sina.com) (M. Dong).

troencephalography (EEG). Significant results obtained by those methods evidenced that each was able to be used as an indicator of pain intensity. However, the former three methods are more expensive and used inconvenience for patients and clinicians. Among those methods, EEG with high temporal resolution is considered as a very useful noninvasive tool for assessing pain intensity. Furthermore, EEG has virtues of clinical convenience, low cost setup and maintenance. In light of EEG advantages, it has gained much interest from experts searching for measures to characterize the perception of pain. By looking at the principles of related methods, some researchers used frequency domain analysis method to analyze the states of pain under different frequency bands of EEG signals, and other researchers combined the feature extraction and machine learning method to classify the level of pain perception.

The frequency domain analysis method depends on utilizing power spectrum characteristics to analyze subjective pain perception. Nir et al. [8] carried out a subjective perception experiment of tonic pain through a thermal contact-heat simulator. The peak alpha frequency (PAF) was used as an objective measure for pain perception. Experimental results showed that the relevance of PAF to the neural processing of tonic pain provided its potential to characterize pain perception. Later, Nir et al. [9] took steps forward this research to focus on exploring the characteristics of subjective perception of tonic pain in alpha-1 power and found that it was able to serve as a direct, objective, and experimentally stable measure for subjective pain perception. Shao et al. [10] investigated electrocortical responses to tonic cold pain with frequency-domain analysis across five frequency bands, i.e., 1–4 Hz, 4–8 Hz, 8–12 Hz, 12–18 Hz, and 18–30 Hz, in multiple brain regions. Experiments demonstrated that there were significantly different 4–8 Hz, 12–18 Hz, and 18–30 Hz source activities between cold pain and no pain conditions. Gram et al. [11] investigated changes in EEG between rest and tonic cold pain. The findings showed that relative spectral indices increased in delta and gamma bands, and decreased in theta, alpha-1 and alpha-2 bands. Chang et al. [12] explored the effects of tonic cold pain in men. Continuous EEG recordings were obtained before, during, and after a cold pressor test. Experimental results showed that a decrease of alpha and increase of beta activities occurred after the onset of cold pressor test. Hansen et al. [13] recorded EEG signals during rest and with a hand immersed in iced water. The experiment was performed in eight frequency bands, i.e., delta (1–4 Hz), theta (4–8 Hz), alpha-1 (8–10 Hz), alpha-2 (10–12 Hz), beta-1 (12–18 Hz), beta-2 (18–24 Hz), beta-3 (24–32 Hz), and gamma (32–60 Hz). Findings showed that reliability was high in all eight frequency bands during rest and cold pressor conditions. Similar works have also shown a decrease in the alpha frequency band and an increase in the beta frequency band [14–20]. Provided methods based on frequency domain analysis have effectively demonstrated that the activity of certain frequency bands was strongly related to pain response, e.g., alpha and beta frequency bands.

Machine learning methods rely on extracting features in the time domain, frequency domain, and time-frequency domain of EEG signals to train a classification model for recognizing different levels of pain perception. Vatankhah and Toliyat [21] proposed wavelet coherency method to estimate pain states. Wavelet coefficients were firstly extracted to provide pain feature vectors, then a hybrid scheme using a Hidden Markov Model (HMM) and a Support Vector Machine (SVM) was utilized for classifying between no-pain and pain states. With fuzzy logic theory, Panavarnan and Wongsawat [22] developed a pain feature extraction algorithm indicated the thermal pain state of the EEG, then a polynomial kernel support vector machine classifier was used for classifying two states of pain. Akin this method, Kumar et al. [23] designed an EEG model based on fuzzy sets for pain estimation and observed that EEG parameters 'Hjorth Activity' and 'Spectral Entropy' could

reflect the level of pain experienced by the surgical patient during the postoperative period. Vijayakumar et al. [24] developed a robust and accurate machine learning method for quantifying tonic thermal pain. Using time-frequency wavelet representations of independent components a random forest model was trained to predict pain scores. The proposed method assessed the relative importance of each frequency band to pain quantification. Conclusions demonstrated that the gamma band was the most important to classification accuracy. Hadjileontiadis et al. [25] designed an approach that combined the continuous wavelet transform (CWT) with higher-order statistics (HOS) for extracting tonic cold pain representations in EEG signals with five frequency bands. The experimental results, based on SVM, Quadratic Discriminant Analysis (QDA), Mahalanobis (MAH), and k-Nearest Neighbors (k-NN) classifiers, showed that the WHOS-based features successfully discriminated the relaxed state from the pain state (mild and severe pain). Alazrai et al. [26] present an EEG-based approach, which was employed to identify four different tonic cold pain states, i.e., relaxed state, relaxed-to-pain state (RPS), pain state (PS), and pain-to-relaxed state (PRS). Using discrete wavelet transform, time-frequency representations of EEG signals were first extracted to construct nonlinear features. A proposed two-layer hierarchical classification framework that was successfully able to identify four pain states. Compared with the frequency domain analysis method, machine learning method is better able to discriminate objective pain states, since the features not only come from frequency domain, but also time variation of the pain-related EEG characteristics.

Although machine learning methods achieved better classification results of pain states, the features used for training a classifier were still hand-engineered. We believe handcrafted features are not able to extract enough feature representations from pain EEG signals. Recently, deep learning is a branch of machine learning that takes advantage of multiple layers of linear and non-linear processing units to learn hierarchical representations of features from input data. It can be seen as an end-to-end learning method which identifies unseen examples without the need for feature engineering. Especially, Convolutional Neural Networks (ConvNets) as a predominant method of deep learning have been successfully used in brain-signal decoding [27–34]. ConvNets can extract and learn local, low-level features from EEG data by using convolutions, which are key components, and then form global and high-level features in deeper layers. Motivated by the recent and widespread success of ConvNets in EEG signals, this paper introduces a new framework for tonic cold pain classification based on deep ConvNets, which is different from the existing works that develop dedicated algorithms to extract features from EEG data of pain perception. To the best of our knowledge, there is no existing work describing deep ConvNets systems that cope with identifying pain states.

Based on frequency domain analysis method, we learned that obvious changes between pain and no pain states occurred in certain frequency bands, e.g., alpha and beta. Inspired by these phenomena, specifically, we develop a classification framework that utilizes several ConvNet branches, each of which is charge of one frequency band, extracting time-invariant features from EEG data of pain perception. Then extracted features on different frequency bands are concatenated together and fed into the last fully-connected network which outputs three types of pain states, i.e., No Pain, Moderate Pain, and Severe Pain. This study assesses the tonic pain under the innocuous cold stimuli condition, which is built with the iced water simulation experiment. Works has been previously demonstrated that the human brain was able to perceive distinct cold (or hot) somatic stimulation and discriminate its intensity with different affective responses [8,9,35]. In this experiment, we recruited thirty-two subjects and collected EEG

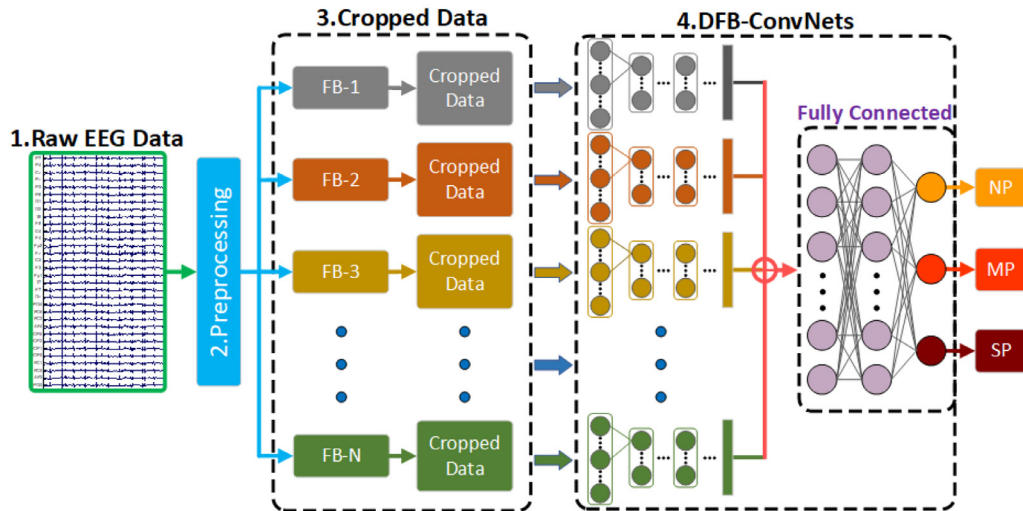


Fig. 1. The overall flowchart of the proposed architecture for tonic cold pain assessment, FB-N represents for the Nth frequency band.

data from each subject under tonic cold pain stimuli conditions. Experimental results demonstrated that the proposed method outperformed existing state-of-the-art classifiers. Therefore, the aim of this work is to develop a better approach using deep learning algorithms to objectively assess pain states. It could be taken as a promising candidate for the development of an expert system for clinical pain application.

In summary, the main contributions of this paper are as follows: (1) A novel ConvNets framework with end-to-end learning is proposed for tonic pain states classification. (2) The joint representation using diverse frequency band in the proposed framework can simultaneously take advantages of more temporal representations from different frequency bands of EEG signals. (3) In the first convolutional block of the proposed framework, a specific architecture with two layers, i.e., temporal convolution and spatial filter, is designed for better handle the large number of input channels for EEG signals. (4) A completed experimental procedure is designed for innocuous tonic cold pain stimulation.

The rest of this paper is organized as follows. The method used in our research is described in Section 2. Section 3 presents the process of experimental design and experimental datasets establishment. Experimental results are reported in Section 4. Finally, in Section 5, discussion and conclusions are given.

## 2. The proposed method

The architecture of the proposed tonic cold pain assessment method is illustrated in Fig. 1. It mainly consists of four successive modules: (1) raw EEG data acquisition module (See Section 3.1); (2) preprocessing module; (3) cropped data module; and (4) diverse frequency band-based Convolutional Neural Networks (DFB-ConvNets) module. All training and testing EEG data used in this method from our experimental data (See Section 3.3).

Specifically, the preprocessing module aims to remove noise signals from raw EEG data. Then, specified frequency bands are filtered with a band-pass Butterworth filter. The cropped data module performed on each frequency band is used to increase samples for training and testing DFB-ConvNets. Its aim is to avoid overfitting usually caused by limited data. The diverse frequency band-based ConvNets module is utilized to extract feature representations from different frequency bands of EEG signals, and then further to recognize different pain states. To be specific, the EEG data on each frequency band is first sent into a single ConvNet branch (also called pipeline), which is used to extract different features. Then, the architecture of multiple ConvNet branches with each

one representing a frequency band, so which is called diverse frequency band-based ConvNets (DFB-ConvNets) model, is proposed to identify pain states. In each ConvNets model, the deep feature extractor respectively performs convolutional operations in order to extracting temporal representations from preprocessed EEG data. Lastly, all features derived from different frequency bands are concatenated and fed into the last fully-connected network which performs classification. In this paper, the proposed method is able to classify the pain into three categories, i.e., No Pain (NP), Moderate Pain (MP), and Severe Pain (SP).

### 2.1. Preprocessing

EEG activity is contaminated by strong muscle, eye movements, and eye blinks, which is a serious problem for EEG interpretation and analysis. Therefore, the prediction of pain perception would rely on advanced signal processing techniques. In our research, three steps were carried out to preprocess EEG raw data. Firstly, EEG signals contaminated with strong muscle artifacts were manually rejected by visual inspection. Then, an independent component analysis (ICA) algorithm used in this pipeline can separate and remove eye blinks and eye movements by line decomposition. As described by Jung et al. [46], artifacts related to eye-blinks and movements could be automatically identified based on the combination of stereotyped artifact specific spatial and temporal features. In our research, the artifact components were selected through analyzing scalp topographies of independent components obtained by an EEGLAB toolbox in MATLAB 2018. Two useful heuristics were taken as two criterions for removing the independent components: (1) Eye movements should project mainly to frontal sites with a lowpass time course; (2) Eye blinks should project to frontal sites and have large punctate activations. After eliminating artifact components, the remaining independent components were used to reconstruct the denoised EEG trails. Lastly, all EEG signals were filtered with a 6th order digital Butterworth bandpass filter with different ranges of cutoff frequencies, i.e., [1Hz–4 Hz], [4Hz–8 Hz], [8Hz–13 Hz], [13Hz–30 Hz], and [30Hz–49 Hz]. The five passbands correspond to delta, theta, alpha, beta, and gamma frequency bands, respectively.

### 2.2. The cropped data

This work adopts a cropped strategy applied in EEG data of pain, which is able to lead to many more samples for training and testing deep ConvNets [36]. According to Section 3.4, obtained

continuous EEG signal for each subject is cut into three segments with each one belongs to a type of pain state. In our study, we assume that each subject  $i$  has an EEG pain dataset, which is separated into labeled time-segments of the cropped EEG data.

Concretely, given an origin pain dataset  $\mathbf{D}_i = \{(\mathbf{X}_1, \mathbf{y}_1), \dots, (\mathbf{X}_{N_i}, \mathbf{y}_{N_i})\}$ , where  $N_i$  denotes the total number of cropped EEG signals for subject  $i$ . The input matrix  $\mathbf{X}_j \in \mathbb{R}^{E \times T}$  of trail  $j$ ,  $1 \leq j \leq N_i$  contains the preprocessed signals of  $E$ -recorded electrodes and  $T$ -discretized time steps,  $\mathbf{y}_{N_i}$  is the class label, where takes values from a set of three class labels. It can be expressed as:

$$\forall \mathbf{y}_{N_i} : \mathbf{y}_{N_i} \in L = \{l_1 = \text{"no pain"}, l_2 = \text{"moderate pain"}, l_3 = \text{"severe pain"}\} \quad (1)$$

In our work, we select a segmented pain signal of 1 s as one crop on each pain state (Sampling rate: 500 Hz). Then,  $\mathbf{X}_j$  is composed of 500 sampling points of EEG data. Lastly, all of those crops are used as new training samples and have the same label  $\mathbf{y}_{N_i}$ .

More formally, one crop, corresponding to one second EEG data, namely contains 500 EEG data points as sampling period of this system is 2 milliseconds. The stride size, in our case, is set as one. In other words, the size of one second EEG data is selected as a sliding window, it moved with equal stride size on EEG data  $\mathbf{X}_{N_i}$ . Overall, this results in 29,501 crops on 60 s EEG data (See Section 3.4), which corresponds to each pain state. Generally, the ConvNets have no differences between crops and the global temporal structure of the features in the complete trail, which stands for a segmented EEG data. Hence, the goal of using the cropped strategy is to force the ConvNets into extracting as many features as possible that are present in all crops of EEG data from each pain state.

### 2.3. DFB-ConvNets

As discussed in the introduction, frequency-based analysis method demonstrated that EEG activity of pain perception had obvious distinction in form of power value between no pain and pain states at certain frequency bands, e.g., alpha and beta. In addition, machine learning-based experimental results also showed that best accuracy of pain recognition occurred in alpha and beta frequency bands [22,25,26]. However, current methods for analyzing EEG pain data and recognizing pain states were only performed in a single frequency band. Inspired by discrete wavelet transform (DWT) for representing EEG signals [37], which analyzes an input signal at different frequency bands with different resolutions by decomposing the signal into coarse detail and approximation information, a DFB-ConvNets model is designed. It is able to extract more information of pain features from diverse frequency bands of EEG signals and further to fuse those to obtain better classification results.

#### 2.3.1. Specific details

All frequency bands we have specified are taken as input data for the proposed DFB-ConvNets model in Fig. 1. We employ multiple deep ConvNets where each one corresponds to one frequency band in our model to extract diverse pain representations from EEG signals. In the proposed framework, each ConvNet has the same architecture, which consists of five convolution-max-pooling blocks, as illustrated in Fig. 2. A specific first block is designed for dealing with the input data, followed by four standard convolution-max-pooling blocks and a flatten layer. After that, the flattened features are sent into the concatenation operation, which is used to fuse diverse features derived from other pipelines. Lastly, the concatenated features are fed into the last fully-connected network which performs classification.

Except for the first block (detailed below), each block has two layers: convolution and pooling. Specifically, each convolutional

**Table 1**  
Parameters of the ConvNets architecture in FB-1.

Layers	Type	Number of neurons	Filter size	Stride
Block 1	Temporal Conv1	$32 \times 488 \times 25$	$1 \times 13$	1
	Spatial Filter	$1 \times 488 \times 25$	$32 \times 1$	1
	Max-pooling	$1 \times 244 \times 25$	$1 \times 2$	2
Block 2	Conv2	$1 \times 232 \times 50$	$1 \times 13$	1
	Max-pooling	$1 \times 116 \times 50$	$1 \times 2$	2
Block 3	Conv3	$1 \times 104 \times 100$	$1 \times 13$	1
	Max-pooling	$1 \times 72 \times 100$	$1 \times 2$	2
Block 4	Conv4	$1 \times 60 \times 200$	$1 \times 13$	1
	Max-pooling	$1 \times 30 \times 200$	$1 \times 2$	2
Block 5	Conv5	$1 \times 18 \times 400$	$1 \times 13$	1
	Max-pooling	$1 \times 18 \times 400$	$1 \times 9$	9
Flatten Layer	–	$400 \times 1 \times 2$	–	–

layer performs three operations sequentially: 1D-convolution (One dimension-convolution) with its filter, batch normalization, and applying the rectified linear unit activation (ReLU) which is expressed as:

$$\text{relu}(x) = \max(0, x) = \begin{cases} x, & \text{if } x > 0 \\ 0, & \text{if } x \leq 0 \end{cases} \quad (2)$$

where  $x$  is the input of activation function.

For each pooling layer, its aim is to down sample the input data with the max operation. The specifications of the number of neurons, filter size, and stride in each layer are summarized in Table 1. In each block, the convolutional block respectively shows the number of filters, a filter size, and a stride size. The pooling block respectively shows a pooling size and a stride size. Dropout operations are performed to all convolutional layers with a probability of 0.5.

The first block is split into three layers: temporal convolution, spatial filter, and max pooling. The architecture of the first block is shown in Fig. 3. Compared to the RGB-images (RGB stands for Red, Green, and Blue colors) with three input channels (one per color), we consider the EEG data as a 32-channel data, i.e., one input channel per electrode. The goal of the proposed architecture is better to deal with the large number of input channels for EEG signals.

In the first layer, each filter with size  $1 \times 13$  performs a convolution on each input channel. After performing a series of convolving operations with the input EEG data, twenty-five feature maps of size  $32 \times 488$  are created. In the second layer, each feature map corresponds to the previous feature map in the first layer. Hence, the same number of feature maps is formed through the spatial filtering with weights, which performs on all possible pairs of electrodes. In this block, the activation function is not performed in between the first and second layers, but operated in the secondary layer. Lastly, performing a max pooling with  $1 \times 2$  area is followed by the activation operation.

After obtaining diverse features of all specified frequency bands by aforementioned feature extraction operations, those representative features are further fused together. Specifically, the features from different pipelines are concatenated with others to obtain a feature vector  $\mathbf{f}$ , which is defined as:

$$\mathbf{f} = \{\mathbf{f}_{\text{FB-1}}, \mathbf{f}_{\text{FB-2}}, \dots, \mathbf{f}_{\text{FB-N}}\} \quad (3)$$

where FB-N denotes different frequency bands,  $\mathbf{f}_{\text{FB-N}}$  represents the extracted feature vector corresponding to a frequency band.

Then, the concatenated feature vector is fed into a fully-connected layer, as illustrated in Fig. 1. Finally, a softmax layer is applied to predict the classification label of the pain state.

#### 2.3.2. DFB-ConvNets training

As for our proposed model, it is trained in the supervised classification setting. Hence, the DFB-ConvNets needs to compute a



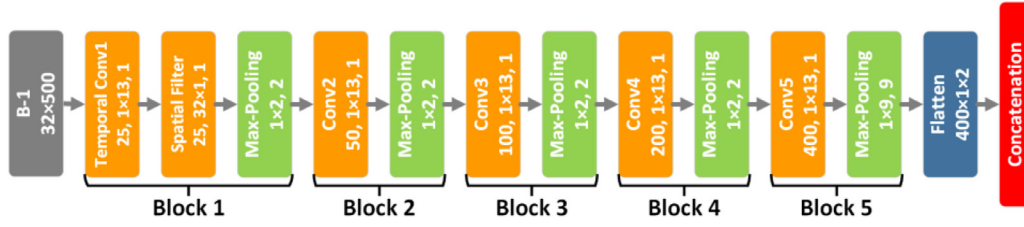


Fig. 2. The architecture of the FB-N ConvNets branch with five blocks. Color code used: orange = convolution, green = max pooling, blue = flatten, red = concatenation.

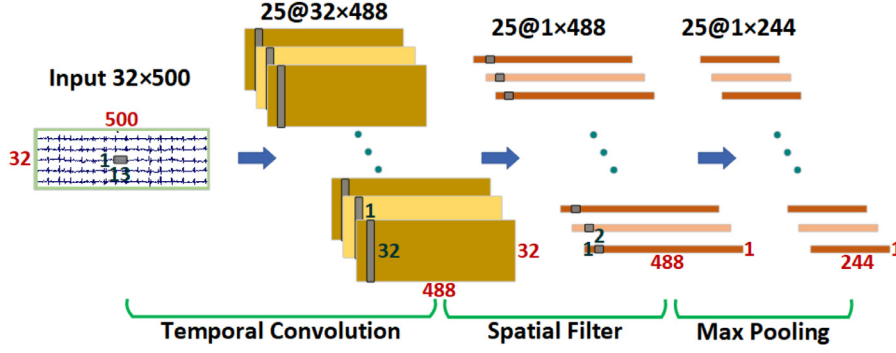


Fig. 3. The architecture of the first block.

function from input data to one real number per class:  $f(\mathbf{X}_j; \theta)$ :  $R^{E \cdot T} \rightarrow R^M$ , where  $\theta$  are the parameters of the function  $f$ ,  $E$  is the number of electrodes,  $T$  is the number of timesteps, and  $M$  is the number of output labels (pain states),  $j$  is the sample. To train the DFB-ConvNets model, the output is transformed to conditional probabilities of a label  $l_m$  given the input  $\mathbf{X}_j$  with the softmax function:

$$p(l_m | f_m(\mathbf{X}_j; \theta)) = \frac{\exp(f_m(\mathbf{X}_j; \theta))}{\sum_{k=1}^M \exp(f_k(\mathbf{X}_j; \theta))} \quad (4)$$

Then, we can train the DFB-ConvNets model to assign highest probabilities to the correct labels by minimizing the error function:

$$\theta^* = \arg \min_{\theta} \frac{1}{N} \sum_{j=1}^N L(y_j, p(l_m | f_m(\mathbf{X}_j; \theta))) \quad (5)$$

where  $L$  denotes the cross-entropy function:

$$L(y_j, p(l_m | f_m(\mathbf{X}_j; \theta))) = - \sum_{m=1}^M q(y_j = l_m) \log p(l_m | f_m(\mathbf{X}_j; \theta)) \quad (6)$$

where  $q(y_j = l_m)$  denotes the value of true label corresponds to the  $m$ -th output.

In our case, the Adam method, which is a variant of stochastic gradient decent, is used for optimizing the parameters via back-propagation [39].

Compared with conventional machine learning methods for pain states classification, which computes can be viewed as consisting of a feature extraction function and a classifier function, the ConvNets can learn both jointly. The ConvNets is especially useful for large datasets as it is able to learn valuable features which may be unknown discriminative features. Specifically, for complex EEG data, some unknown representative features could not be used by more traditional feature extraction methods. Moreover, our proposed DFB-ConvNets model is capable of learning more unknown representative features of continuous pain EEG signals from different pipelines of frequency bands.

### 3. Experimental procedure and data

To collect and store experimental data, firstly, the apparatus and experimental procedure are presented. Then, the pain intensity ratings across the subjects are given. Lastly, the obtained data are divided into training, validating and testing sets for the proposed DFB-ConvNets model.

#### 3.1. Experimental setup

In our work, we use the Enobio 32-electrode EEG wireless recording system (Neuroelectronics Inc., Barcelona, Spain) to record the EEG signals across the subjects. The captured data is streamed through the standard Bluetooth ISM (Industrial Scientific Medical) band, operating distance range is 10 m. The electrodes are inserted and arranged in the cap (Neuroelectrical cap) according to the international 10–10 system. The recorded scalp sites include P7, P4, Cz, Pz, P3, P8, O1, O2, T8, F8, C4, F4, Fp2, Fz, C3, F3, Fp1, T7, F7, Oz, PO4, FC6, FC2, AF4, CP6, CP2, CP1, CP5, FC1, FC5, AF3, and PO3 positions. The scalp electrodes are referenced to a pair of electrodes which are connected to CMS and DRL channels. The system was digitized at a sampling rate of 500 Hz.

#### 3.2. Experimental procedure

Thirty-two subjects, twenty female and twelve males, aged from 19–35 years, took part in this experiment. All were right-handed, not on any medications, and without any history of neurological and psychiatric disease. The whole experimental process was completed within five days. Specifically, in the first day, each participating subject familiarised with the experimental details. Then, a series of stimulation experiments was carried out in next three days. The purpose was to determine the tolerable time of one hand submerged in iced water. During those experiments, EEG signals did not need to be captured. The last day, we formally launched the experiment for capturing the EEG data from each subject with the same experimental procedure. The detailed process of the experiment is described as follows.

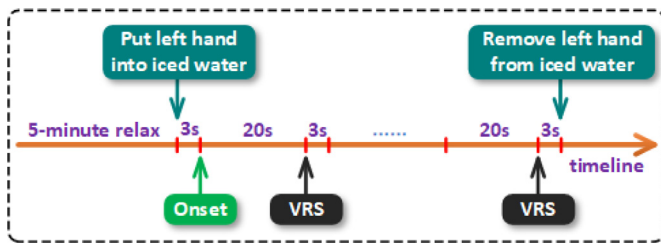


Fig. 4. Illustration of the experimental procedure.

Each subject with eyes open was comfortably seated in an upright chair with a distance of 1 m from a computer screen. The diagram of experimental process in a trail is shown in Fig. 4. Concretely, each subject was first given 5-minute to relax prior to the initiation of a trail. Then the subject was asked to put his/her left hand into a barrel with iced water mixture ( $3^{\circ}\text{C} \pm 0.5^{\circ}\text{C}$ ) in order to give the tonic cold stimuli. Followed the first 3 s was spent on keeping the subject's hand still in iced water to simplify the process of removing the muscular artifacts caused by hand movements when preprocessing. After 3 s, the tonic cold stimuli experiment was beginning. All subjects were required to remain as still as possible and to focus their sight on a displaying green dot in order to minimize muscular and occipital artifacts.

During the experiment, a 3-second break was given to each subject in order to rate the perceived pain intensity on 11-point (0–10) verbal rating scales (VRSs, 0: no pain, 1: barely noticeable pain, 5: mild pain and 10: worst pain ever). The aforementioned experimental procedure was repeated until the subject felt the pain became unbearable.

All subjects were from Northeastern University, Boston, USA, and the experimental procedure was approved by the Northeastern University Institutional Review Board (IRB). Other subjects were volunteers from Beijing Institute of Technology and gave written informed consent prior to the beginning of the experiments.

### 3.3. Experimental data

From the results of the simulated experiment, we observed that the tolerable time of the subject's hand submerged in iced water was 210 s, i.e., nine times to rate scores of pain perception, which was able to be accepted by all subjects. In our case, the proposed method is capable of classifying three types of pain states, i.e., No Pain (0), Moderate Pain (1–5), and Severe Pain (6–10), respectively. We randomly selected 16 subjects' pain scores from the participants as shown in Fig. 5. For no pain state, i.e., No Pain (0), we extracted the EEG data from the relax phase prior to the initiation of each trail, which was used as no pain measurement.

Then, the EEG data for each subject was partitioned into three segments, which correspond to three types of pain signals, i.e., no pain, moderate pain and severe pain, respectively. For each pain state, we determined to extract three 20 s length of EEG data. In our work, the size of one sample was set as 1 s EEG data. Hence, 30,000 sampling points (Sampling frequency: 500 Hz) was created for each pain state. Lastly, using the cropped strategy (See Section 2.2), EEG data for each state was further processed to establish the dataset of pain states. The preprocessing data were completed in MATLAB 2018. The proposed DFB-ConvNets model was developed in Tensorflow 1.10 with Python 3.6.

### 3.4. N-fold Cross-validation

To assess the generalization capability and choose optimal parameters of one classification method, the N-fold cross-validation method is used in our work. Specifically, the set corresponding to

**Table 2**  
Confusion matrix for three-class classification.

		Predicted pain labels		
		NP	MP	SP
True pain labels	NP	$x_{11}$	$x_{12}$	$x_{13}$
	MP	$x_{21}$	$x_{22}$	$x_{23}$
	SP	$x_{31}$	$x_{32}$	$x_{33}$

each pain state is first divided into N subsets. Then, the N-1 subsets are used as the training set and the remaining subset is used as the testing set. The training process of each model candidate is performed iteratively N times. Further, the classification accuracies of N folds are averaged. The best model is determined by the optimal parameters with the best average validation result. Lastly, the optimal pair of parameters is used to train the model on all the training data.

By the aforementioned strategy, the 10-fold stratified cross-validation approach is used for parameters optimization of our proposed DFB-ConvNets model. More formally, considering to the lower mean square and bias, we decide to perform ten rounds of 10-fold stratified cross-validation on the all dataset. Firstly, the dataset corresponding to each pain state is divided into 10 subsets with equal data size. In each round, then, nine out of ten subsets are utilized for the 10-fold cross-validation procedure, and the left one subset is used for testing. This process is repeated 10 times until all EEG signals are included. Its aim is to enable a different subset used as the testing data in each time. The classification performance across all ten rounds of testing for each subject is averaged for the final experimental results.

## 4. Experimental results

To test the performance of the tonic cold pain recognition, this section gives the experimental results obtained by our proposed DFB-ConvNets model on the EEG database. Section 4.1 introduces the evaluation method by means of generalized confusion matrix strategy. Section 4.2 reports the results of performance evaluation on testing DFB-ConvNets model with different combinations of frequency bands. A comparison between the DFB-ConvNets model and the Single Frequency Band-based ConvNets (SFB-ConvNets) model is carried out in Section 4.3. Section 4.4 discusses the experimental results obtained using the conventional machine learning methods. The last subsection analyzes and discusses comparison results between our proposed method and existing machine learning methods on identifying the tonic cold pain states.

### 4.1. Evaluation method

Our proposed model is attributed to a three-class classifier consisting of no pain (NP), moderate pain (MP), and severe pain (SP). Its performance is evaluated using a generalized confusion matrix (also called an error matrix) which is a table where each row represents the cases in an actual class and each column represents the cases in a predicted class in term of the DFB-ConvNets model. In our paper, based on statistical information of confusion matrix, the average testing accuracy, precision, specificity, sensitivity, and F-1 measure are calculated as performance evaluation metrics over the ten train-test repetition [38].

Table 2 shows the format of the confusion matrix with three classes. Firstly, three one-vs-all confusion matrices for each class  $C_i$  ( $i = 1, 2, 3$ ) need to be calculated [38]. Then, for an individual class, the assessment is defined by  $TP_i$ ,  $FN_i$ ,  $TN_i$ , and  $FP_i$ . The  $Precision_i$ ,  $Specificity_i$ ,  $Sensitivity_i$ ,  $F1_i$  metrics for  $C_i$ , and the accuracy of the

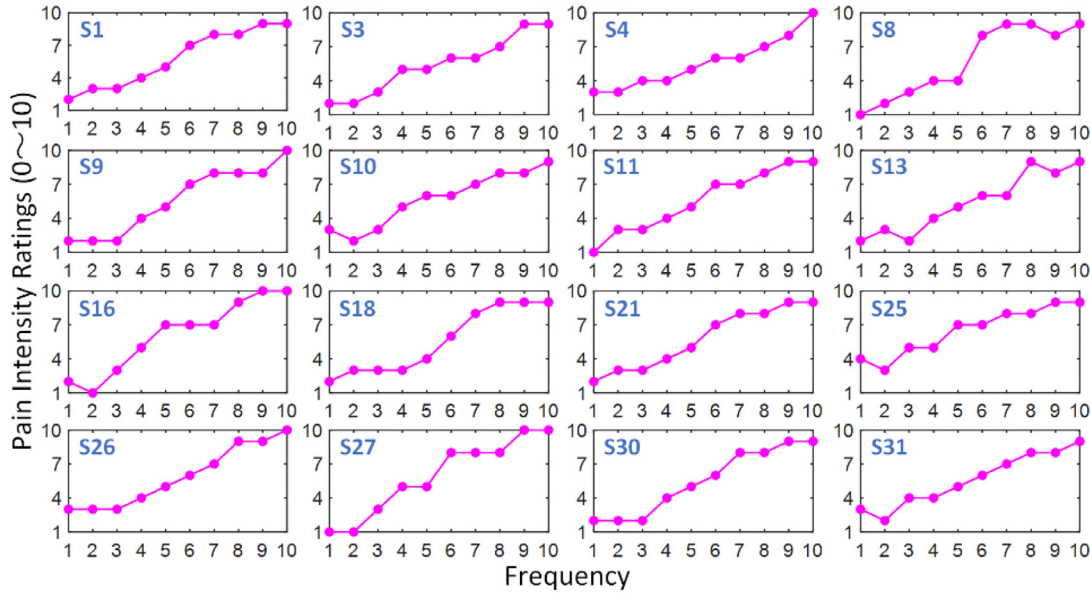


Fig. 5. Selected 16 Pain intensity ratings from 32 subjects.

proposed classifier can be expressed as follows:

$$Precision_i = \frac{TP_i}{TP_i + FP_i} \quad (7)$$

$$Specificity_i = \frac{TN_i}{TN_i + FP_i} \quad (8)$$

$$Sensitivity_i = \frac{TP_i}{TP_i + FN_i} \quad (9)$$

$$F1_i = \frac{2}{Sensitivity_i^{-1} + Precision_i^{-1}} \quad (10)$$

$$Accuracy = \frac{\sum_{i=1}^3 TP_i}{N} \quad (11)$$

where  $TP_i = x_{ij}$  denotes total number of true-positive cases for  $C_i$ ,  $TN_i = \sum_{j=1}^3 \sum_{k \neq i} x_{jk}$  denotes total number of true-negative cases for  $C_i$ ,  $FP_i = \sum_{j=1}^3 x_{ji}$  denotes total numbers of false-positive cases for  $C_i$ , and  $FN_i = \sum_{j=1}^3 x_{ji}$  denotes total numbers of false-negative cases for  $C_i$ ,  $N$  is the total number of samples for each test.

#### 4.2. Results on diverse frequency bands

In our case, five frequency bands are utilized for analyzing tonic cold pain states. Those frequency bands can be represented as  $\delta$  (delta),  $\theta$  (theta),  $\alpha$  (alpha),  $\beta$  (beta), and  $\gamma$  (gamma), respectively. To validate our proposed diverse frequency bands strategy, the aforementioned frequency bands are combined with each other non-repeatedly. The obtained twenty combinations of frequency bands are showed in Table 3. To simplify representation, the CN ( $N = 1, \dots, 20$ ) stands for combinations of different frequency bands.

Then, we compute and evaluate the performance of the proposed DFB-ConvNets model on twenty combinations of frequency bands. The precision, specificity, sensitivity, and F1-measure for each combination are averaged across all subjects, respectively. The obtained evaluation metrics for tonic cold pain states identification are listed in Tables 4 and 5. Specifically, Table 4 shows the performance results of C1 to C10, Table 5 lists ones of C11 to C20. From Table 4, we observe that the best performance is obtained on

Table 3

Combinations of different frequency bands.

Name	Frequency bands	Name	Frequency bands
C1	$\delta, \theta$	C11	$\theta, \alpha$
C2	$\delta, \alpha$	C12	$\theta, \beta$
C3	$\delta, \beta$	C13	$\theta, \gamma$
C4	$\delta, \gamma$	C14	$\theta, \alpha, \beta$
C5	$\delta, \theta, \alpha$	C15	$\theta, \alpha, \gamma$
C6	$\delta, \theta, \beta$	C16	$\theta, \alpha, \beta, \gamma$
C7	$\delta, \theta, \gamma$	C17	$\alpha, \beta$
C8	$\delta, \theta, \alpha, \beta$	C18	$\alpha, \gamma$
C9	$\delta, \theta, \alpha, \gamma$	C19	$\alpha, \beta, \gamma$
C10	$\delta, \theta, \alpha, \beta, \gamma$	C20	$\beta, \gamma$

C10, which consists of five frequency bands, with overall average precision, specificity, sensitivity, and F1-measure of 87.58%, 93.72%, 87.43%, and 87.43%. Compared with performance results obtained in Table 5, C19 is higher than C10. The overall average precision, specificity, sensitivity, and F1-measure are 96.05%, 98.03%, 96.06%, and 96.05%, respectively.

Fig. 6 shows the average recognition accuracy for each combination in the proposed classification framework. The best accuracy of identifying pain states is 97.37% with standard deviation 0.26% using the C19, which is composed of alpha, beta, and gamma bands. Compared with C19, we observe that the C18 has a slightly lower accuracy result which is 96.26%. It is interesting to note that the classification accuracy drops slightly when the gamma band is ignored. Additionally, C17 also obtains a closer classification accuracy of 96.17% with respect to C18. Based on those results, it is seen that the alpha, beta, and gamma bands contribute most to classification accuracy, and that the gamma band has a certain effect on classification performance of identifying tonic cold pain states. Hence, the results state that the combination of alpha, beta, and gamma bands seems to be important to pain quantification.

#### 4.3. Comparison with SFB-ConvNets model

Our proposed framework is evaluated on different combinations of frequency bands of EEG signals. Its aim is to extract various feature representations from different frequency bands, which have a better ability to classify the pain states. For this task, it can also

**Table 4**  
Results of identifying the tonic cold pain states on C1 to C10.

Combination	Pain state	Precision (%)	Specificity (%)	Sensitivity (%)	F1-measure (%)
C1	NP	69.96	84.68	71.35	70.65
	MP	63.10	79.40	70.47	66.58
	SP	78.46	90.70	67.75	72.71
C2	NP	72.58	85.74	76.50	74.63
	MP	68.83	83.82	71.45	70.12
	SP	74.71	88.47	68.12	71.27
C3	NP	75.10	87.39	77.59	76.32
	MP	68.95	82.67	76.67	72.61
	SP	76.52	89.78	65.54	70.61
C4	NP	70.41	84.68	72.90	71.63
	MP	64.67	79.90	73.59	68.84
	SP	77.45	90.68	64.02	70.10
C5	NP	77.76	88.86	77.95	77.85
	MP	70.04	84.11	72.46	72.09
	SP	79.52	90.40	74.53	76.94
C6	NP	74.40	86.59	77.98	83.72
	MP	75.03	87.70	73.91	83.10
	SP	77.17	89.97	74.61	84.18
C7	NP	72.04	84.87	77.96	74.88
	MP	71.30	85.05	74.26	72.75
	SP	84.35	93.14	73.92	78.79
C8	NP	73.37	85.51	79.85	76.47
	MP	73.05	86.18	74.94	73.98
	SP	84.17	92.99	74.57	79.08
C9	NP	78.11	88.24	83.95	80.92
	MP	75.93	87.60	78.22	77.06
	SP	85.88	93.68	76.87	81.13
<b>C10</b>	<b>NP</b>	<b>85.88</b>	<b>92.55</b>	<b>90.53</b>	<b>88.14</b>
	<b>MP</b>	<b>85.72</b>	<b>92.67</b>	<b>88.06</b>	<b>86.88</b>
	<b>SP</b>	<b>91.13</b>	<b>95.93</b>	<b>83.71</b>	<b>87.26</b>

**Table 5**  
Results of identifying the tonic cold pain on C11 to C20.

Combination	Pain state	Precision (%)	Specificity (%)	Sensitivity (%)	F1-measure (%)
C11	NP	78.22	88.83	80.23	79.21
	MP	78.12	89.08	77.97	78.45
	SP	79.13	89.82	77.25	78.18
C12	NP	80.61	90.19	81.62	81.11
	MP	75.67	87.19	79.68	77.62
	SP	83.47	92.28	78.01	80.65
C13	NP	65.82	80.77	74.07	69.70
	MP	67.89	83.91	68.06	67.98
	SP	77.71	90.28	67.79	72.41
C14	NP	90.82	95.19	95.14	92.93
	MP	90.45	95.04	93.89	92.13
	SP	96.25	98.28	88.02	91.95
C15	NP	91.87	95.82	94.60	93.22
	MP	92.38	96.09	94.95	93.65
	SP	93.79	97.07	88.40	91.01
C16	NP	91.70	95.17	94.87	93.26
	MP	91.40	95.54	94.85	93.09
	SP	94.66	97.52	87.82	91.11
C17	NP	93.56	96.67	96.63	95.07
	MP	93.48	96.69	94.91	94.19
	SP	95.82	98.01	91.21	93.46
C18	NP	93.70	96.76	96.30	94.98
	MP	94.40	97.18	95.17	94.79
	SP	95.13	97.65	91.72	93.39
<b>C19</b>	<b>NP</b>	<b>95.10</b>	<b>97.46</b>	<b>98.39</b>	<b>96.71</b>
	<b>MP</b>	<b>96.27</b>	<b>98.16</b>	<b>94.74</b>	<b>95.50</b>
	<b>SP</b>	<b>96.87</b>	<b>98.46</b>	<b>95.05</b>	<b>95.95</b>
C20	NP	91.43	95.55	95.10	93.23
	MP	91.77	95.77	94.44	93.09
	SP	94.35	97.37	87.82	90.96

be evaluated on a single frequency band. Actually, many previous works of analyzing and identifying tonic cold pain states were operated in a single frequency band. In order to validate the performance of diverse frequency bands strategy, we compare the classification results of our proposed model with the single frequency band-based Convolutional Neural Networks (SFB-ConvNets) model.

More specifically, one branch of the proposed DFB-ConvNets is used to perform the pain classification on a single frequency band of EEG signals, i.e.,  $\delta$ ,  $\theta$ ,  $\alpha$ ,  $\beta$ , and  $\gamma$ , respectively. The structure of SFB-ConvNets is composed of five convolution-max-pooling blocks, as illustrated in Fig. 2. In this model, the concatenation layer is not required. The extracted features by five blocks are



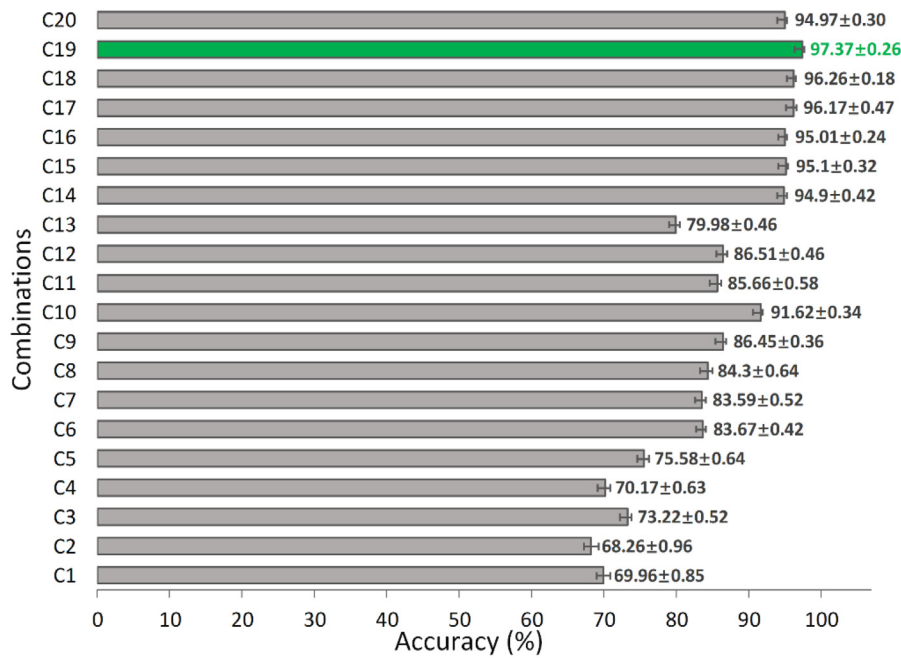


Fig. 6. Average accuracy of each combination in the proposed classification framework.

Table 6

Comparison of classification performance with the SFB-ConvNets model.

Frequency band	Pain state	Precision (%)	Specificity (%)	Sensitivity (%)	F1-measure (%)
<b>C19</b>	<b>NP</b>	<b>95.10</b>	<b>97.46</b>	<b>98.39</b>	<b>96.71</b>
	<b>MP</b>	<b>96.27</b>	<b>98.16</b>	<b>94.74</b>	<b>95.50</b>
	<b>SP</b>	<b>96.87</b>	<b>98.46</b>	<b>95.05</b>	<b>95.95</b>
delta	NP	63.75	80.83	67.44	65.54
	MP	66.34	78.82	64.46	62.33
	SP	68.66	86.30	60.00	64.04
theta	NP	64.51	81.18	68.43	66.41
	MP	65.39	82.06	67.79	66.57
	SP	66.46	84.86	59.98	63.66
alpha	NP	88.94	94.16	94.43	91.60
	MP	90.74	95.34	90.25	90.49
	SP	93.32	96.87	88.06	90.62
beta	NP	90.20	95.04	91.35	90.77
	MP	89.99	94.90	91.62	90.80
	SP	92.80	96.51	89.93	91.34
gamma	NP	88.81	94.47	87.82	88.31
	MP	86.64	92.97	91.21	88.87
	SP	91.26	95.81	87.46	89.32

directly sent into the fully-connected layer to perform classification task.

Table 6 lists the obtained metrics for tonic cold pain states identification using precision, specificity, sensitivity, and F1-measure. It is obvious that the experimental result of C19 has greater classification performance compared with other frequency bands, which illustrates that the fusion strategy can surely be improved. As a consequence, the proposed DFB-ConvNets model achieves the best accuracy for that it has more feature representations with consideration of multiple possible frequency bands.

Fig. 7 illustrates the average classification accuracies of C19 in our proposed model and five frequency bands in the SFB-ConvNets model. It is apparent when the SFB-ConvNets model is performed on  $\alpha$  and  $\beta$  bands, the obtained classification performance is close, i.e., 93.94% and 93.98%. For  $\gamma$  band, it achieves 92.55% of classification accuracy, which is a slightly worse than  $\alpha$  and  $\beta$  bands. These results are consistent with findings reported in previous pain studies based on frequency domain analysis and machine learning methods. More specifically, for frequency domain analysis method, the EEG in  $\beta$  band was found to increase significantly under cold

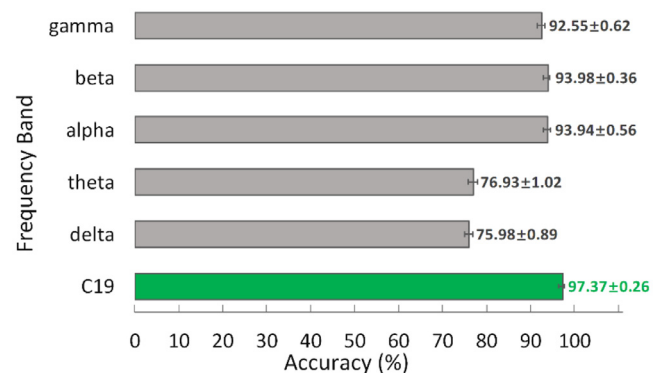


Fig. 7. Average accuracies of C19 in the proposed framework and five frequency bands in the SFB-ConvNets model.

pain conditions [8,9]. For machine learning methods, the classification results in  $\alpha$  and  $\beta$  bands are better than other frequency

**Table 7**The results of paired *t*-test performed on DFB-ConvNets and SFB-ConvNets classifiers.

Paired <i>t</i> -test	C19 vs. delta	C19 vs. theta	C19 vs. alpha	C19 vs. beta	C19 vs. gamma
<i>p</i> -value	$4.645 \times 10^{-17}$	$1.266 \times 10^{-19}$	$2.055 \times 10^{-6}$	$6.088 \times 10^{-5}$	$1.131 \times 10^{-9}$

bands [22,25,26]. Based on these results obtained in this case, it is evident that  $\alpha$ ,  $\beta$ , and  $\gamma$  bands contribute the most effective feature representations to classification results of identifying tonic cold pain states.

In our research, a paired *t*-test is used to compare the DFB-ConvNets and SFB-ConvNets classifiers which are applied to 32 subjects (same subjects). The *p*-value of the paired *t*-test carried out on the accuracy results are shown in Table 7. It can be observed that there is significant difference in the accuracy between the DFB-ConvNets and each SFB-ConvNets with  $p = .000$  at significance level,  $\alpha = 5\%$ . Therefore, there is strong evidence that the DFB-ConvNets classifier does lead to improvements of pain states classification.

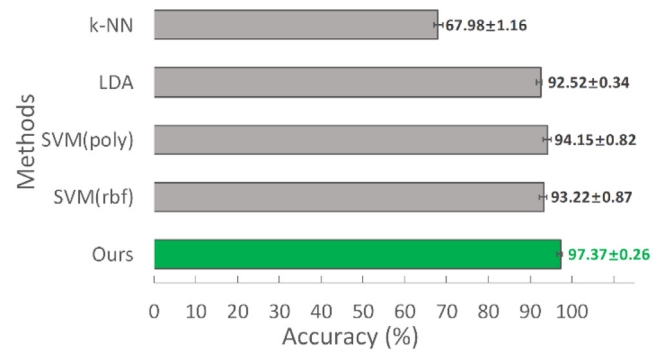
#### 4.4. Comparison with other classifiers

To prove the efficiency of the proposed ConvNets framework, a comparison between the proposed method with the three classifiers, i.e., Support Vector Machines (SVM), Linear Discriminant Analysis (LDA) and k-Nearest Neighbors (k-NN), is carried out. The above-mentioned classifiers are attributed to traditional machine learning methods, which are primarily designed for the binary classification problem. In our research, however, a three-class classifier is required to be built for classifying no pain (NP), moderate pain (MP), and severe pain (SP). Therefore, the one-versus-one scheme were used in the traditional classifiers. These classifiers were performed using the Scikit Learn Toolkit in Python.

For the traditional machine learning algorithms, it depends on extracting features which are used to train a classifier for performing classification task. As discussed in the introduction, the Wavelet transform algorithm is a usual feature extraction method for pain states classification. Here, a previous work for solving four-class motor imagery, i.e., combined Wavelet analysis and Common Spatial Pattern (CSP) method, was used in this work as a feature extraction method [45]. The preprocessed EEG signals would be decomposed by Wavelet Transform. In our research, a six-layer Wavelet Transform was applied to EEG signals. According to the rules of the decomposition, the sub-frequency bands should be [0, 3.906], [3.906, 7.8125], [7.8125, 15.625], [15.625, 31.25], [31.25, 62.5], [62.5, 125], and [125, 250]. Because the frequency bands of [7.8125, 15.625], [15.625, 31.25], and [31.25, 62.5] include  $\alpha$ ,  $\beta$ ,  $\gamma$  bands, the related wavelet coefficients corresponding to the three frequency bands should reflect their frequency characteristics. Then each channel of sampling values was replaced by the wavelet coefficients as the input of CSP. The feature vectors from CSP calculation are used to train the three classifiers. The detailed information about this method can be seen in [45].

The parameters for the three classifiers are given here. For SVM, polynomial (poly) and radial basis function (rbf) are used as its kernel functions. The penalty parameter *C* is set as 2.3 and the degree of poly as 3. For LDA, the automatic shrinkage using the Ledoit-Wolf lemma is taken as parameters shrinkage and least squares solution as solver. For k-NN, the number of nearest neighbors were chosen as 5, 10, 20, 40, and 50. Through experiments, with 40 nearest neighbors higher accuracy was achieved.

Table 8 lists the classification performance of the DFB-ConvNets model and the three classifiers. Obviously, our proposed DFB-ConvNets method produces the highest results in each metric. Fig. 8 shows the classification accuracies of five classifiers. It is

**Fig. 8.** Average accuracies of our proposed framework and conventional machine learning methods.

worth highlighting that our method achieves the high accuracy while k-NN classifier produces the worst result. The reasons may be attributed to why the conventional classifier is not able to produce higher accuracies than our method as follows: (1) The traditional machine learning method commonly perform good with binary class data. (2) The better performance largely depends on the selection of appropriate feature set representing the EEG signals. Table 9 gives the *p*-value of the paired *t*-test carried out on the accuracy results. It can be seen that there is significant difference in the accuracy between the DFB-ConvNets and each conventional classifier with  $p = .000$  at significance level,  $\alpha = 5\%$ . Therefore, there is strong evidence that the DFB-ConvNets classifier improve the performance of pain states classification.

#### 4.5. Comparison with state-of-the-art methods

According to aforementioned classification results, we choose the C19 with best performance of identifying tonic cold pain states as our optimal framework to compare with some state-of-the-art classification approaches based on machine learning strategy, which are described earlier. For the sake of fairness, all of approaches are performed on our established dataset. In addition to [22], other methods totally use the discrete wavelet transform to construct a time-frequency representation of the EEG signal for extracting a set of nonlinear features. More specifically, the chosen methods were evaluated on different frequency bands as shown in Table 10. Refs. [26,25,22] are run on a single frequency band, i.e.,  $\beta$  or  $\alpha$ , [24] on the whole frequency bands, i.e.,  $\delta$ ,  $\theta$ ,  $\alpha$ ,  $\beta$ , and  $\gamma$ , and [21] on the four frequency bands, i.e.,  $\delta$ ,  $\theta$ ,  $\alpha$ , and  $\beta$ .

Table 10 lists the classification performance of six approaches using precision, specificity, sensitivity, and F1-measure as an evaluation metrics. It can be seen that the classification performance based on our proposed DFB-ConvNets model is better than that based on wavelet transform approach, and obviously superior to that based on Fuzzy logic approach.

Fig. 9 illustrates the classification accuracies of six approaches. We can easily find that classification result of our proposed framework is slightly higher than that of [24] and [26], which obtain 97.07% and 96.89%, respectively. The lowest classification performance (i.e., 71.84%) is achieved by [22], nearly 26% lower than that of our method. Considering a possible reason for this case, we think it can be attributed to difficult to construct an appropriate fuzzy rule set. The paired *t*-test has been carried out on the re-

**Table 8**

Comparison of classification performance with the conventional machine learning methods.

Methods	Pain state	Precision (%)	Specificity (%)	Sensitivity (%)	F1-measure (%)
Our method	NP	<b>95.10</b>	<b>97.46</b>	<b>98.39</b>	<b>96.71</b>
	MP	<b>96.27</b>	<b>98.16</b>	<b>94.74</b>	<b>95.50</b>
	SP	<b>96.87</b>	<b>98.46</b>	<b>95.05</b>	<b>95.95</b>
SVM (rbf)	NP	90.25	94.97	95.22	90.18
	MP	90.12	95.14	93.76	91.90
	SP	95.78	98.07	88.35	91.92
SVM (poly)	NP	91.76	95.60	94.80	93.26
	MP	92.56	95.98	94.70	93.62
	SP	92.87	97.12	88.20	90.47
LDA	NP	85.47	91.79	90.26	87.80
	MP	84.97	91.87	87.56	86.25
	SP	91.05	95.83	83.24	86.97
k-NN	NP	72.36	85.67	77.37	74.78
	MP	68.97	83.76	69.96	69.46
	SP	75.12	87.98	69.57	72.24

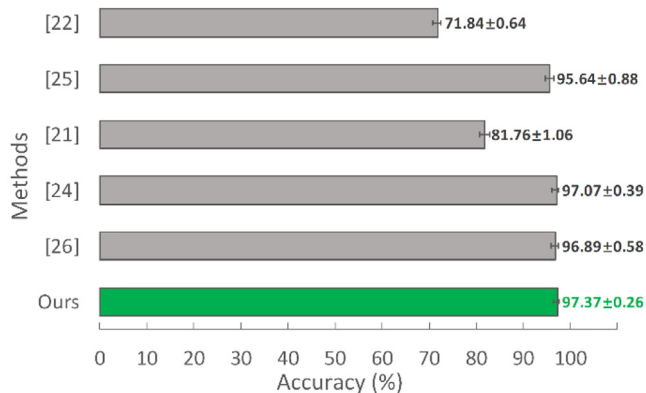
**Table 9**The results of paired *t*-test performed on DFB-ConvNets classifier and the conventional machine learning methods.

Paired <i>t</i> -test	Ours vs. SVM(rbf)	Ours vs. SVM(poly)	Ours vs. LDA	Ours vs. k-NN
<i>p</i> -value	$3.337 \times 10^{-8}$	$3.313 \times 10^{-9}$	$8.261 \times 10^{-12}$	$1.376 \times 10^{-20}$

**Table 10**

Comparison of classification results of identifying tonic cold pain with the state-of-the-art methods.

Method	Frequency band	Pain state	Precision (%)	Specificity (%)	Sensitivity (%)	F1-measure (%)
<b>Our Method</b>	$\alpha, \beta, \gamma$	NP	<b>95.10</b>	<b>97.46</b>	<b>98.39</b>	<b>96.71</b>
		MP	<b>96.27</b>	<b>98.16</b>	<b>94.74</b>	<b>95.50</b>
		SP	<b>96.87</b>	<b>98.46</b>	<b>95.05</b>	<b>95.95</b>
[26]	$\beta$	NP	93.93	96.84	97.89	95.87
		MP	95.82	97.95	93.72	94.75
		SP	96.37	98.22	94.42	95.39
[24]	$\delta, \theta, \alpha, \beta, \gamma$	NP	94.27	97.01	98.26	96.22
		MP	96.12	98.10	93.88	94.99
		SP	96.52	98.29	94.68	95.59
[21]	$\delta, \theta, \alpha, \beta$	NP	71.47	84.45	77.92	74.55
		MP	72.91	89.95	75.61	74.23
		SP	73.78	88.56	64.39	68.77
[25]	$\beta$	NP	92.47	96.06	96.84	94.61
		MP	93.44	96.77	92.00	92.72
		SP	94.55	97.36	91.52	93.01
[22]	$\alpha$	NP	58.05	78.07	60.71	59.35
		MP	53.94	74.95	58.67	56.20
		SP	62.23	83.63	53.92	57.78

**Fig. 9.** Average accuracies of our proposed framework and the state-of-the-art methods.

sults listed in Table 11. For [21,25,22], it can be observed that there are significant differences compared with the DFB-ConvNets classifier, obtained  $p = .000$  at significance level,  $\alpha = 5\%$ . For [26] and

[24], however, there are no differences compared with the DFB-ConvNets classifier, obtained  $p = .0680$  and  $p = .2037$  at significance level,  $\alpha = 5\%$ . Therefore, there is no strong evidence that the DFB-ConvNets classifier can improve the performance of pain states classification.

## 5. Discussion and conclusions

The conventional practice to classify the pain states is by using frequency domain analysis methods and traditional machine learning algorithms. Frequency domain analysis-based methods are not automatic algorithms to recognize pain states, but they provide evidence that there are obvious changes between pain and no pain states occurred in specific frequency bands, e.g., alpha and beta. Traditional machine learning algorithms are able to obtain better classification results of pain states, but those depend on extracted features used for training a classifier which are still hand-engineered. In this case, not enough feature representations are extracted from pain EEG signals. To overcome the aforementioned limitations, in this paper, a diverse frequency band-based ConvNets model is proposed for tonic cold pain states classification.

**Table 11**The results of paired *t*-test performed on DFB-ConvNets classifier and the state-of-the-art methods.

Paired <i>t</i> -test	Ours vs. [26]	Ours vs. [24]	Ours vs. [21]	Ours vs. [25]	Ours vs. [22]
<i>p</i> -value	0.0680	0.2037	$5.133 \times 10^{-16}$	0.0002	$8.461 \times 10^{-18}$

The proposed framework first extracted diverse feature representations from different frequency bands, then these features were concatenated and fed into a fully-connected network which performed pain states classification. To verify this purpose of the study, 32 subjects were recruited and a procedure of cold stimuli simulation experiment was designed and performed for collecting EEG data, which was used for training and testing our proposed model. The advantage of DFB-ConvNets comes from utilization of diverse frequency band-based input and exploration of abundant feature representations of EEG signals with the deep neural network structure. Experimental results demonstrate that the proposed DFB-ConvNets model is able to provide higher accuracy than state-of-the-art techniques.

Although the proposed framework is able to perform the pain states classification well and shows a competitive accuracy compared to the state-of-the-art methods, the experiments and results in this paper are subjected to some limitations: (1) All results mentioned in this paper are subject to the execution in a specific environment. (2) The proposed DFB-ConvNets model is currently limited to performing the cold pain state classification, results may be different with pain states due to disease. (3) A limited dataset with only 32 subjects is used in our research. Overall, the proposed framework contributes with an alternative way to the endeavor toward object quantification of the subjective characterization of tonic pain.

### Declaration of Competing Interest

The authors declare that they have no conflict of interest.

### Acknowledgement

This work was supported by Program for Changjiang Scholars and Innovative Research Team in University [grant number IRT\_16R07], National Natural Science Foundation of China [grant number 51705024]; U.S. National Science Foundation (NSF) [grant number 1838796]. We thank all the participants who have participated in this work.

### References

- [1] J.S. Shieh, C.Y. Dai, Y.R. Wen, W.S. Sun, A novel fuzzy pain demand index derived from patient-controlled analgesia for postoperative pain, *IEEE Trans. Biomed. Eng.* 54 (2007) 2123–2132, doi:10.1109/TBME.2007.896584.
- [2] C. Schnakers, N.D. Zasler, Pain assessment and management in disorders of consciousness, *Curr. Opin. Neurol.* 20 (2007) 620–626, doi:10.1097/WCO.0b013e3282f169d9.
- [3] K. Herr, P.J. Coyne, M. McCaffery, R. Manworren, S. Merkel, Pain assessment in the patient unable to self-report: position statement with clinical practice recommendations, *Pain Manag. Nurs.* 12 (2011) 230–250, doi:10.1016/j.pmn.2011.10.002.
- [4] D.D. Price, Psychological and neural mechanisms of the affective dimension of pain, *Science* 288 (2000) 1769–1772, doi:10.1126/science.288.5472.1769.
- [5] P.M. Aslaksen, I.N. Myrbakk, R.S. Høifødt, M.A. Flaten, The effect of experimenter gender on autonomic and subjective responses to pain stimuli, *Pain* 129 (2007) 260–268, doi:10.1016/j.pain.2006.10.011.
- [6] M.M. Kamdar, Principles of analgesic use in the treatment of acute pain and cancer pain, *J. Palliat. Med.* 13 (2010) 217–218, doi:10.1089/jpm.2010.9854.
- [7] T.D. Walsh, Practical problems in pain measurements, *Pain* 19 (1984) 96–98.
- [8] R.R. Nir, A. Sinai, R. Einat, E. Sprecher, D. Yarnitsky, Pain assessment by continuous EEG: association between subjective perception of tonic pain and peak frequency of alpha oscillations during stimulation and at rest, *Brain Res.* 1344 (2010) 77–86, doi:10.1016/j.brainres.2010.05.004.
- [9] R.R. Nir, A. Sinai, R. Moont, E. Harari, D. Yarnitsky D, Tonic pain and continuous EEG: prediction of subjective pain perception by alpha-1 power during stimulation and at rest, *Clin. Neurophysiol.* 123 (2012) 605–612, doi:10.1016/j.clinph.2011.08.006.
- [10] S.Y. Shao, K.Q. Shen, K. Yu, E.P.V. Wilder-Smith, X.P. Li, Frequency-domain EEG source analysis for acute tonic pain perception, *Clin. Neurophysiol.* 123 (2012) 2042–2049, doi:10.1016/j.clinph.2012.02.084.
- [11] M. Gram, C. Graversen, S.S. Olesen, A.M. Drewes, Dynamic spectral indices of the electroencephalogram provide new insights into tonic pain, *Clinical* 126 (2015) 763–771, doi:10.1016/j.clinph.2014.07.027.
- [12] P.F. Chang, L. Arendt-Nielsen, C.A.N. Chen, Dynamic changes and spatial correlation of EEG during cold pressor test in man, *Brain Res. Bull.* 57 (2002) 667–675, doi:10.1016/S0304-9230(01)00763-8.
- [13] T.M. Hansen, E.B. Mark, S.S. Olesen, M. Gram, J.B. Frøkjær, A.M. Drewes AM, Characterization of cortical source generators based on electroencephalography during tonic pain, *J. Pain Res.* 7 (2017) 1401–1409, doi:10.2147/JPR.S132909.
- [14] M. Steriade, P. Gloor, R.R. Linás, F.H.L.D. Silva, M.M. Mesulam, Basic mechanisms of cerebral rhythmic activities, *Electroencephalogr. Clin. Neurophysiol.* 76 (1990) 481–508, doi:10.1016/0013-4694(90)90001-Z.
- [15] F.L.D. Silva, Neural mechanisms underlying brain waves: from neural membranes to networks, *Electroencephalogr. Clin. Neurophysiol.* 79 (1991) 81–93, doi:10.1016/0013-4694(91)90044-5.
- [16] M. Backonja, E.W. Howland, J. Wang, J.L. Smith, M. Salinsky, C.S. Cleeland, Tonic changes in alpha power during immersion of the hand in cold water, *Electroencephalogr. Clin. Neurophysiol.* 79 (1991) 192–203, doi:10.1016/0013-4694(91)90137-S.
- [17] P.F. Chang, L.A. Nielsen, T.G. Nielsen, P. Svensson, C.A.N. Chen, Topographic effects of tonic cutaneous nociceptive stimulation on human electroencephalograph, *Neurosci. Lett.* 305 (2001) 49–52, doi:10.1016/S0304-3940(01)01802-X.
- [18] A.C.N. Chen, S.F. Dworkin, J. Huang, J. Gehrig, Topographic brain measures of human pain and pain responsivity, *Pain* 37 (1989) 129–141, doi:10.1016/0304-3959(89)90125-5.
- [19] A.C.N. Chen, S.D. Dworkin, J. Huang, J. Gehrig, Human pain responsivity in a tonic pain model: psychological determinants, *Pain* 37 (1989) 143–160, doi:10.1016/0304-3959(89)90126-7.
- [20] S. Ferracuti, S. Seri, D. Mattia, G. Cruccu, Quantitative eeg modifications during the cold water pressor test: hemispheric and hand differences, *Int. J. Psychophysiol.* 17 (1994) 261–268, doi:10.1016/0167-8760(94)90068-X.
- [21] M. Vatankhah, A. Toliyat, Pain level measurement using discrete wavelet transform, *Inte. J. Eng. Technol.* 8 (2016) 380–384, doi:10.7763/IJET.2016.V8.917.
- [22] P. Panavaranan, M. Wongsawat, EEG-Based pain estimation via fuzzy logic and polynomial kernel support vector machine, in: *Proceedings of the Biomedical Engineering International Conference*, 2013, doi:10.1109/BMEiCon.2013.6687668.
- [23] S. Kumar, A. Kumar, A. Trikha, S. Anand, Electroencephalogram based quantitative estimation of pain for balanced anesthesia, *Measurement* 59 (2015) 296–301, doi:10.1016/j.measurement.2014.09.021.
- [24] V. Vijayakumar, M. Case, S. Shirinipour, B. He B, Quantifying and characterizing tonic thermal pain across subjects from eeg data using random forest models, *IEEE Trans. Biomed. Eng.* 64 (2017) 2988–2996, doi:10.1109/TBME.2017.2756870.
- [25] L.J. Hadjileontiadis, EEG-Based tonic cold pain characterization using wavelet higher order spectral features, *IEEE Trans. Biomed. Eng.* 62 (2015) 1981–1991, doi:10.1109/TBME.2015.2409133.
- [26] R. Alazrai, M. Momani, H.A. Khudair, M.I. Daoud, EEG-based tonic cold pain recognition using wavelet transform, *Neural Comput. Appl.* (2017) 1–14, doi:10.1007/s00521-017-3263-6.
- [27] A. Antoniadis, L. Spyrou, C.C. Took, S. Sane, Deep learning for epileptic intracranial EEG data, in: *Proceedings of the IEEE 26th International Workshop on Machine Learning for Signal Processing (MLSP)*, 2016, pp. 1–6, doi:10.1109/MLSP.2016.7738824.
- [28] M. Hajjinoroozi, Z. Mao, T. Lin, Y. Huang, EEG-based prediction of driver's cognitive performance by deep convolutional neural network, *Signal Process. Image Commun.* 47 (2016) 549–555, doi:10.1016/j.image.2016.05.018.
- [29] J. Liang, R. Lu, C. Zhang, F. Wang, Predicting seizures from electroencephalography recordings: a knowledge transfer strategy, in: *Proceedings of the IEEE International Conference on Healthcare Informatics (ICHI)*, 2016, pp. 184–191, doi:10.1109/ICHI.2016.27.
- [30] Z. Tang, C. Li, S. Sun S, Single-trail eeg classification of motor imagery using deep convolutional neural networks, *Int. J. Light Electron Opt.* 130 (2017) 11–18, doi:10.1016/j.ijleo.2016.10.117.
- [31] Y.R. Tabar, U. Halici, A novel deep learning approach for classification of EEG motor imagery signals, *J. Neural Eng.* 14 (2016) 016003, doi:10.1088/1741-2560/14/1/016003.



- [32] P. Thodoroff, J. Pineau, A. Lim, Learning robust features using deep learning for automatic seizure detection, in: *Proceedings of the Machine Learning and Healthcare Conference (MLHC)*, 2016, pp. 178–190.
- [33] S. Stober, D.J. Cameron, J.A. Grah, Using convolutional neural networks to recognize rhythm stimuli from electroencephalography recordings, in: *Proceedings of the 27th International Conference on Neural Information Processing Systems*, 2014, pp. 1449–1457.
- [34] X. Sun, C. Qian, Z. Wu, B. Luo, G. Pan, Remembered or forgotten?—an EEG-Based computational prediction approach, *PLoS ONE* 11 (2016) e0167497, doi:10.1371/journal.pone.0167497.
- [35] P.F. Chang, L. Arendt-Nielsen, C.A.N. Chen, Comparative cerebral responses to non-painful warm vs. cold stimuli in man: EEG power spectra and coherence, *Int. J. Psychophysiol.* 55 (2005) 73–83, doi:10.1016/j.ijpsycho.2004.06.006.
- [36] R.T. Schirmmeister, J.T. Springenberg, L.D.J. Fiederer, M. Glasstetter, K. Eggenberger, M. Tangermann, F. Hutter, W. Burgard, T. Ball, Deep learning with convolutional neural networks for eeg decoding and visualization, *Hum. Brain Mapp.* 38 (2017) 5391–5420, doi:10.1002/hbm.23730.
- [37] A.N. Akansu, R.A. Haddad, *Multiresolution Signal decomposition: transforms, subbands, and Wavelets*, Academic Press, Cambridge, 2001.
- [38] D.M.W. Powers, Evaluation: from precision, recall and F-measure to ROC, informedness, markedness and correlation, *J. Mach. Learn. Technol.* 2 (2011) 37–63, doi:10.9735/2229–3981.
- [39] D.P. Kingma, J. Ba, Adam: a method for stochastic optimization, in: *Proceedings of the 3rd International Conference on Learning Representations*, 2014.
- [40] D.P. Vittorio, F. Stefano, S. Umberto, P. Patrizia, C. Giorgio, L.L. Gian, A cerebral blood flow study on tonic pain activation in man, *Pain* 56 (1994) 167–173, doi:10.1016/0304-3959(94)90091-4.
- [41] P. Petrovic, K.M. Petersson, P.H. Ghatan, S. Stone-Elander, M. Ingvar, Pain-related cerebral activation is altered by a distracting cognitive task, *Pain* 85 (2000) 19–30, doi:10.1016/S0304-3959(99)00232-8.
- [42] M. Ingvar, Pain and functional imaging, *Philos. Trans. R. Soc. B* 354 (1999) 1347–1358, doi:10.1098/rstb.1999.0483.
- [43] H.K. Beecher, Experimental pharmacology and measurement of the subjective responses, *Science* 15 (1952) 157–162, doi:10.1126/science.116.3007.157.
- [44] E.S. Berner, M.L. Graber, Overconfidence as a cause of diagnostic error in medicine, *Am. J. Med.* 121 (2008) 2–23, doi:10.1016/j.amjmed.2008.01.001.
- [45] X.P. Bai, X.Z. Wang, S.H. Zheng, M.X. Yu, The offline feature extraction of four-class motor imagery EEG based on ICA and Wavelet-CSP, in: *Proceedings of the 33rd Chinese Control Conference*, 2014, pp. 7189–7194, doi:10.1109/ChiCC.2014.6896188.
- [46] T.P. Jung, S. Makeig, M. Westerfield, J. Townsend, E. Courchesne, T.J. Sejnowski, Removal of eye activity artifacts from visual event-related potentials in normal and clinical subjects, *Clin. Neurophysiol.* 111 (2000) 1745–1758.



**Lianqing Zhu** received his M.S. degree and his Ph.D. in Hefei University of Technology in 1989, and in Harbin Institute of Technology in 2013, respectively.

Now he is a professor and Ph.D. supervisor in Beijing Information Science and Technology University. His main research directions include soft robotics, sensing technology and optical measurement.



**Yingzi Lin** obtained the Ph.D. degree in mechanical engineering from University of Saskatchewan, Saskatoon, SK, Canada, and another Ph.D. degree in vehicle engineering from China Agricultural University, Beijing, China.

She is an Assistant Professor with Department of Mechanical and Industrial Engineering, Northeastern University, Boston, MA, where she directs the Intelligent Human-Machine Systems Laboratory. Her research has been funded by the National Science Foundation, Natural Sciences and Engineering Research Council of Canada, and industries. Her area of expertise includes: driver-vehicle systems, human-centered intelligent machine systems, and human machine interface design.

She is the Chair of the Virtual Environments Technical Group of the Human Factors and Ergonomics Society (HFES). She is on the committees of the Transportation Research Board (TRB) of the National Academy of Sciences.



**Xiaoying Tang** obtained the Ph.D. degree in Electronic Engineering from Beijing Institute of Technology, China.

She is a Professor with School of life Sciences, Beijing Institute of Technology, China, where she directs Biomedical Engineering Laboratory. Her research has been funded by the Natural Science Foundation of China, National 863 program, and industries. Her area of expertise includes: neural networks, biomedical image and signal processing, fMRI brain functional imaging, and pattern recognition.



**Yikang Guo** received his B.S. and M.Sc. degree from School of Electronic and Information Engineering, Beijing Jiaotong University, Beijing, China, and School of Automation, Beijing Institute of Technology, Beijing, China, respectively.

Currently he is pursuing toward the doctoral degree in Northeastern University, Boston, USA. His research interests include neural networks, pattern recognitions, and human-brain interaction.



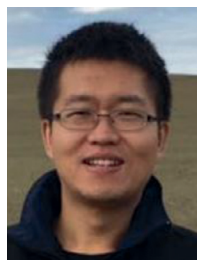
**Guangkai Sun** received his B.Sc. degree in 2007 and M.Sc. degree in 2010 from Hebei University of Science and Technology, received his Ph.D. degree in 2015 from Beihang University.

Now he is an associate professor in the School of Instruments Science and Opto-Electronic Engineering at Beijing Information Science and Technology University. His main research interests include novel optical sensing, visual measurement technologies and soft robotics.



**Mingli Dong** received her M.Sc. degree in 1989 from Hefei University of Technology, received her Ph.D. degree in 2009 from Beijing Institute of Technology.

She is currently a professor in Beijing Information Science & Technology University. Her main research interests include optical fiber sensing, vision measurement technology, precision measurement and instruments.



**Mingxin Yu** received M.S. degree in Electronic Engineering, in 2010, and Ph.D. degree in Control Science & Engineering, in 2015, from Beijing Institute of Technology, Beijing, China.

He has been a visiting research scientist with the Department of Mechanical and Industrial Engineering, Northeastern University, Boston, USA, and a Post-Doctoral Research Fellow with the School of Life Sciences, Beijing Institute of Technology, Beijing, China. Currently he is an associate professor working in the School of Instruments Science and Opto-Electronic Engineering at Beijing Information Science and Technology University, Beijing, China.

His research interests include neural networks, pattern recognitions, image processing, and human-brain interaction. He has published about 15 refereed journal and conference papers in the recent years. Dr. Yu is also the reviewer for many Journals, such as IEEE Transactions on Cybernetics, Journal of Eye Movement Research, et al.



**Yichen Sun** received his bachelor degree from Xi'an Technological University in 2016.

He is currently a graduate student at Beijing Information Science and Technology University, Beijing, China. His research interests include deep learning, optical neural network.

**Bofei Zhu** received his bachelor's degree from Carnegie Mellon University in 2018.

He is currently a visiting scholar working in the School of Instruments Science and Opto-Electronic Engineering at Beijing Information Science and Technology University, Beijing, China. His research interests include deep learning, machine learning, and pattern recognition.